

Relations between morphological settings and vegetation covers in a medium relief landscape of Central Italy

Giovanna Abbate ⁽¹⁾, Rosa Maria Cavalli ⁽²⁾, Simone Pascucci ⁽²⁾,
Stefano Pignatti ⁽²⁾⁽³⁾ and Maurizio Poscolieri ⁽⁴⁾

⁽¹⁾ Dipartimento di Biologia Vegetale, Università degli Studi di Roma «La Sapienza», Roma, Italy

⁽²⁾ Laboratorio Aereo Ricerche Ambientali (LARA), IIA-CNR, Tor Vergata (RM), Italy

⁽³⁾ Istituto di Metodologie per l'Analisi Ambientale (IMAA), CNR, Tito Scalo (PZ), Italy

⁽⁴⁾ Istituto di Acustica O.M. Corbino (IDAC), CNR, Tor Vergata (RM), Italy

Abstract

Morphometric units and vegetation classes were determined by applying two classification methods to the Soratte Mount area, a medium relief structure within the Italian Latium region. The study aims at defining the relationships between vegetation and landform types and highlighting the main morphological characteristics within examined land cover classes. These were the result of the application of a supervised classification method to the first 28 (VIS-NIR) bands of the airborne MIVIS data collected within an extensive survey campaign over Rome Province. The analysis was supported by photo-interpretation of peculiar MIVIS band combinations and by data acquired during field surveys and from a pre-existing vegetation map. The morphometric data were obtained by processing a raster DEM created from topographic maps. These data were processed by means of a new morphometric classification method based on the statistical multivariate investigation of local topographic gradients, calculated along the 8 azimuth directions of each pixel neighbourhood. Such approach quickly estimates the spatial distribution of different types of homogeneous terrain units, emphasizing the impact of erosional and tectonic processes on the overall relief. Mutual relations between morphometric units and vegetation types were assessed by performing a correspondence analysis between the results of the two classifications.

Key words *hyperspectral data – vegetation mapping – geomorphology – classification methods*

1. Introduction

The physical environment is often regarded as one of the most important factors controlling the spatial heterogeneity of the landscape in mountain areas (Bolstad *et al.*, 1998; Hoersch *et al.*, 2002). According to Hoersch *et al.* (2002)

the ecological space of a vegetation type corresponds to its fundamental *niche* and, in contrast to the fundamental, the realised *niche* is defined through interaction with other vegetation types; finally, the actual geographic space of vegetation types or species is caused by natural factors and human impact. The realised *niche* and the geographic space of a vegetation type in a mountain environment is closely related to topographic relief and so landform attributes, such as elevation, slope, aspect and others, are important input parameters for spatial analysis and modelling of vegetation distribution in mountain landscapes. Thus, topography creates a patchwork-like pattern of small scale habitats and realised *niches* within the ecological space. Besides natural environmental factors, the his-

Mailing address: Dr. Simone Pascucci, Laboratorio Aereo Ricerche Ambientali (LARA), IIA-CNR, Via del Fosso del Cavaliere 100, 00133 Tor Vergata (RM), Italy; e-mail: s.pascucci@lara.rm.cnr.it

tory of human impact in terms of agricultural land use and animal husbandry, but also former and recent natural disturbances (rockfall, mudslides, partly related to human impact, thus being only semi-natural disturbance factors), play a major role for the distribution of vegetation types. The actual vegetation distribution is therefore a result of the complex interaction of historic and recent disturbance factors. Nevertheless, in a landscape marked by human impact the overall influence of topography on vegetation types distribution is beyond doubt.

Remotely sensed data have been widely used for assisting in vegetation mapping in the last few years and have proved to be an effective tool (Rogana *et al.*, 2002), offering the possibility of extrapolating mapping results, especially in large and hardly accessible remote areas. Ahmad *et al.* (1992) and Wyatt (2000) also discussed the use and restrictions of remotely

sensed data for vegetation mapping. The landscape shape, which is so strictly connected to vegetation distribution, is analysed by a discipline such as geomorphometry (Nogami, 1995; Pike, 2002), which, in general, can be considered a bridge between the results of the studies based on field analysis and the physical modelling of geomorphic processes (Onorati *et al.*, 1992). Among other applications (Pike, 2002) morphometric parameters, extracted from a DEM (Wood, 1996), were often analyzed to quantitatively compare terrain units (Giles and Franklin, 1998; Hutchinson and Gallant, 2000; Adediran *et al.*, 2004).

Such approach was followed to investigate a medium-high relief area of the Italian Latium region i) by applying two parallel procedures to identify morphometric units and vegetation types and ii) by statistically analyzing mutual relationships. The definition of these relation-

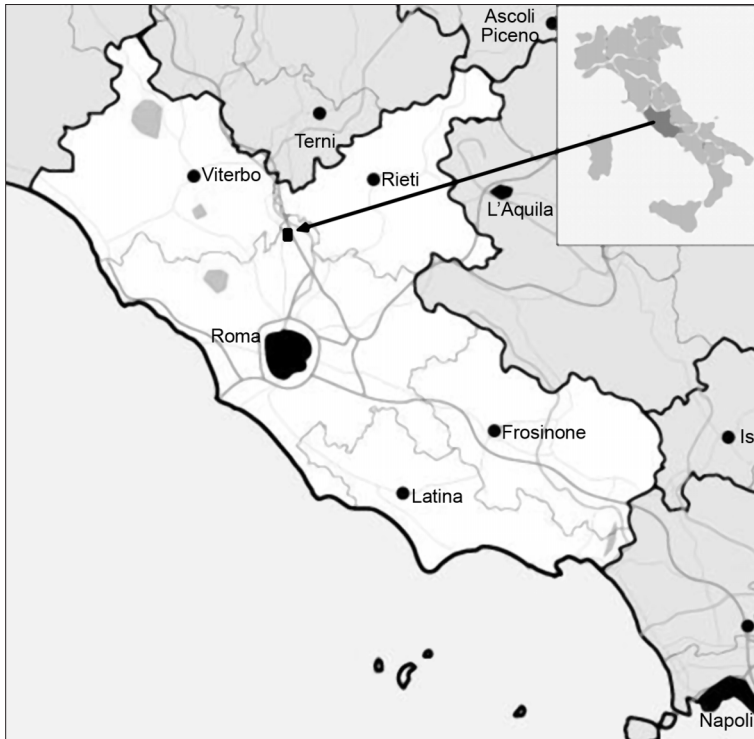


Fig. 1. Location of the study area. On the left the topographic map of the Soratte Mt. on a 1:10.000 scale.

ships and controls highlights the inference of the relative occurrence of land cover types within the morphometric units.

2. Study area

The examined area, centred about the Soratte Mt., is representative of the natural parks of Rome Province's interest, exhibiting carbonate formations, reaching elevations as high as almost 700 m, and peculiar vegetation covers heavily impacted during the 2nd world war (IGM, 1954). The Soratte Mt. is located 40 km north of Rome (fig. 1) and steeply rises over the surrounding landscape as an isolated mountain included inside a natural reserve, which covers a territory of about 410 ha. The main massif exhibits NNW-SSE orientation with a peculiar elliptic shape and reaches a summit of 691 m a.s.l.

The Soratte Mt. is mainly made up of Mesozoic limestone rocks, constituted almost exclusively by formations such as *Calcarea massiccio* and *Corniola*, which were emplaced during the Apennines orogenesis (Miocene) and later underwent extensive faulting, subsequent to the Tyrrhenian Sea's opening (Upper Miocene) (Servizio Geologico d'Italia, 1975). It exhibits steep slopes close to the summit and gently sloping densely vegetated areas along the foothills. The relief has undergone strong karstic erosion activity, especially along the mountain top with the formation of small cavities, leading to surface water flow shortage. Moreover, a hummocky plain, mostly covered by olive trees and crossed by several creeks, encompasses the massif.

The peculiar geomorphological characteristics of the Soratte Mt. and the carbonate bedrock strongly bias the soil types and consequently the

vegetation spatial distribution, clearly diversifying from those of the neighbouring areas (Abbate *et al.*, 1981; Lulli *et al.*, 1988). In the NE side of the massif mixed evergreen and deciduous woods prevail, while in its SW side, where xeric habitats markedly occur, sclerophylls-rich shrublands and thickets are widespread. Dryness conditions take place and the rocky substratum crops out, xerophytic grasslands and garigues predominate. At the foot of the mountain, the lower slant of slopes and deep soils favour the occurrence of deciduous Turkey oak-rich woods. Even in phytoclimatic terms, the study area shows complexity being in the «transition Mediterranean Region», next to the boundary with the «transition Temperate Region» (Blasi, 1994).

3. Data and processing methods

3.1. MIVIS data pre-processing

The vegetation classes have been obtained by applying the Maximum Likelihood (ML) supervised method to the first 28 of 102 hyperspectral bands of the airborne MIVIS (Multi-spectral Infrared Visible Imaging System) data (see table I) collected over Soratte Mt. Such band range (0.4-1.55 μm) was selected because it encompasses the major spectral features related to the biophysical characteristics of the plants; moreover, for the final classification ancillary information about the study area was taken into account. The hyperspectral MIVIS data were acquired during an airborne campaign carried out on 20th June 1998 at an absolute altitude of 1500 m a.s.l.: such value corresponds to elevations varying from 1350 m to 810 m with respect to the topographic surface,

Table I. MIVIS spectral characteristics.

Spectrometer	Spectral region	Bands number	Spectral range (μm)	Band width (μm)
I	Visible	20	0.43-0.83	0.02
II	Near Infrared	8	1.15-1.55	0.05
III	Medium Infrared	64	2.0-2.5	0.009
IV	Thermal Infrared	10	8.2-12.7	0.34-0.54

leading respectively to a pixel ground resolution of 2.7 m and 1.6 m. Recorded data were radiometrically calibrated to radiance ($\text{nWcm}^{-2}\text{sr}^{-1}\mu\text{m}^{-1}$) and geometrically corrected at the CNR ground station seated in Pomezia (Rome, Italy) (Bianchi *et al.*, 1994).

Owing to the morphological complexity of the study area, a raster DEM (10 m/pixel ground resolution) was employed to yield thematic maps topographically corrected. Geometric correction was performed on the basis of re-sampling tables, attained by integrating the airplane's position and attitude data recorded by MIVIS position and attitude system sensors. These tables yielded geocoded thematic maps on the desired scale of 1:10.000, safeguarding the data spectral integrity during this pre-processing phase.

Atmospheric correction procedures were then applied by using the 6S code to correct for the additive path-radiance component.

Another topographic problem affects sensor-perceived radiance: the irradiance received by the target varies with the cosine of the sun-beam incidence angle. The larger the incidence angle, the less the amount of radiation reaching the surface (Teillet *et al.*, 1982): if no other factors change, less electro-magnetic radiance is reflected, as being less received by the target. The instrument perceived radiance is also affected by the sun elevation owing to atmospheric scattering: a lower sun elevation means a longer transportation for the sunbeam and, thus, a larger scattering effect (Ekstrand, 1993). To some extent, the target altitude also has an effect on the sensor registered radiance. This is because the optical thickness of the atmosphere decreases with altitude and also affects the scattering. The amount of radiance reflected by the target depends on the class-specific reflection in different directions, but the class-specific reflection may change with topography if the geometric structure within the class, *e.g.* a forest canopy, changes. Different types of vegetation respond differently to direction and illumination effects (Thomson and Jones, 1990). The relative importance of slope-aspect effects in forest reflectance is still under debate.

Among different topographic correction models, the MIVIS data gathered over Soratte Mt. were processed by applying the *C*-correc-

tion method, which is a modified version of the cosine correction procedure, where a linear relation between radiance and cosine of the incidence angle is assumed. This procedure accounts for the local topographic conditions that influence the direct solar irradiance. To avoid overcorrection, a band specific constant, derived from regression functions between radiance and cosine of the incidence angle, is introduced: it is called *C* and is calculated by dividing the offset of the regression line by the slope.

$$L(\lambda)_{\text{corr}} = L(\lambda)_{\text{uncorr}} * [\cos(z) + C] / [\cos(i) + C]$$

where $C = a/m$; a = offset (intercept) of the regression line; m is the slope (gradient) of the regression line; $\cos i = \cos(e) * \cos(z) + \sin(e) * \sin(z) * \cos(\varphi_s - \varphi_n)$; $L(\lambda)_{\text{uncorr}}$ = spectral radiance measured by sensor ($\text{mWcm}^{-2}\text{sr}^{-1}\mu\text{m}^{-1}$); $L(\lambda)_{\text{corr}}$ = spectral radiance corrected for topography ($\text{mWcm}^{-2}\text{sr}^{-1}\mu\text{m}^{-1}$); i = incidence angle between surface normal and solar beam ($^\circ$); z = solar zenith angle ($^\circ$); e = slope of reference site ($^\circ$); φ_s = solar azimuth angle ($^\circ$); φ_n = slope aspect of reference site ($^\circ$); $\varphi_s - \varphi_n$ = relative azimuth ($^\circ$).

3.2. Land cover data classification

The preliminary analysis was based on the photo-interpretation of the FCC (False Colour Composite) of three MIVIS bands, as pointed out in table II. The 13, 7 and 1 channels (FCC A in table II) respectively represent for vegetation the two bands with higher spectral absorption (Red and Blue) and the one with major reflectivity (Green): this band combination better approaches the natural colour representation. The 19, 28 and 13 channels (FCC B in table II) respectively correspond, instead, to the maximum reflectance plateau in the Near-Infrared, the H_2O absorption peak and chlorophyll absorption peak; hence, this FCC highlights vegetation covers, discriminating between agricultural lands and spontaneous vegetation. Moreover, single MIVIS bands such as 28 ($1.50 < \lambda < 1.55 \mu\text{m}$) and 93 ($8.21 < \lambda < 8.56 \mu\text{m}$) were photo-interpreted to discriminate less easily detectable cov-

Table II. FCC of MIVIS bands.

FCC	Red	Green	Blue
A	Channel 13 ($0.6 < \lambda < 0.69 \mu\text{m}$)	Channel 7 ($0.53 < \lambda < 0.57 \mu\text{m}$)	Channel 1 ($0.43 < \lambda < 0.45 \mu\text{m}$)
B	Channel 19 ($0.79 < \lambda < 0.81 \mu\text{m}$)	Channel 28 ($1.50 < \lambda < 1.55 \mu\text{m}$)	Channel 13 ($0.67 < \lambda < 0.69 \mu\text{m}$)

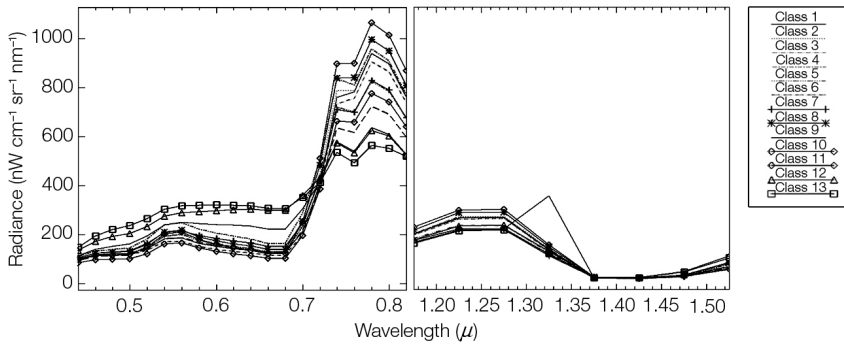


Fig. 2. MIVIS at sensor radiance mean spectra of the 13 Region Of Interest (ROI) relative to the natural environment land cover classes.

ers, such as bare soils, vegetation sparse or in relative dryness conditions.

MIVIS corrected data were further analysed by applying a supervised classification method which needs the collection of the spectral signatures of the main vegetation types.

At first glance, the study area appears mainly exploited for agricultural use with a significant diffusion of olive-trees; there are, however, also wide territory segments characterized by relatively intact natural environment, with well structured woods associated with re-naturalization areas. In particular, the following land use classes were examined and their boundaries outlined: natural environments (woods, thickets, shrublands, grasslands, garigues and rock communities); agricultural lands (arable lands, olive-trees, orchards); urban areas (built-up centres, single dwellings); quarries; water bodies.

By applying appropriate masking procedures, only areas defined as «natural environments» were taken into account in the subsequent investigation. Ancillary information was further provided by carrying out *in situ* surveys to determine the interpretation keys and to ver-

ify the distribution of vegetation types. The results were compared and integrated with those extracted from the pre-existing «Vegetation Map of Soratte Mount» (Abbate *et al.*, 1981).

By considering MIVIS calibrated hyperspectral data and the ancillary information, spectrally homogeneous training areas were selected allowing the definition of an exhaustive number of Regions Of Interest (ROI, as implemented in the ENVI 4.0. software package; RSI, 2003) to be used as input data for the ML supervised classification method. This approach was followed since vegetation types, in the same phenological conditions, exhibit similar spectral trend, but shifted absorption and reflectivity peaks (see fig. 2).

The chosen ROI refer to the following land cover classes:

1. Mediterranean evergreen sclerophylls woods with predominance of *Quercus ilex* (nomenclature of the species follows Pignatti, 1982) and subordinate presence of deciduous trees (*Ostrya carpinifolia*, *Fraxinus ornus*, *Acer monspessulanum*).

2. Mixed woods with evergreen sclerophylls and deciduous trees (*Quercus ilex*, *Ostrya*

carpinifolia, *Fraxinus ornus*, *Acer monspessulanum*).

3. Mixed sclerophylls thickets with deciduous species (*Phillyrea latifolia*, *Quercus ilex*, *Acer monspessulanum*, *Pistacia terebinthus*).

4. Deciduous broadleaf oak-woods with dominance of *Quercus cerris* and subordinately *Quercus frainetto*, *Carpinus orientalis*, *Fraxinus ornus*, *Acer campestre*, *Ostrya carpinifolia*.

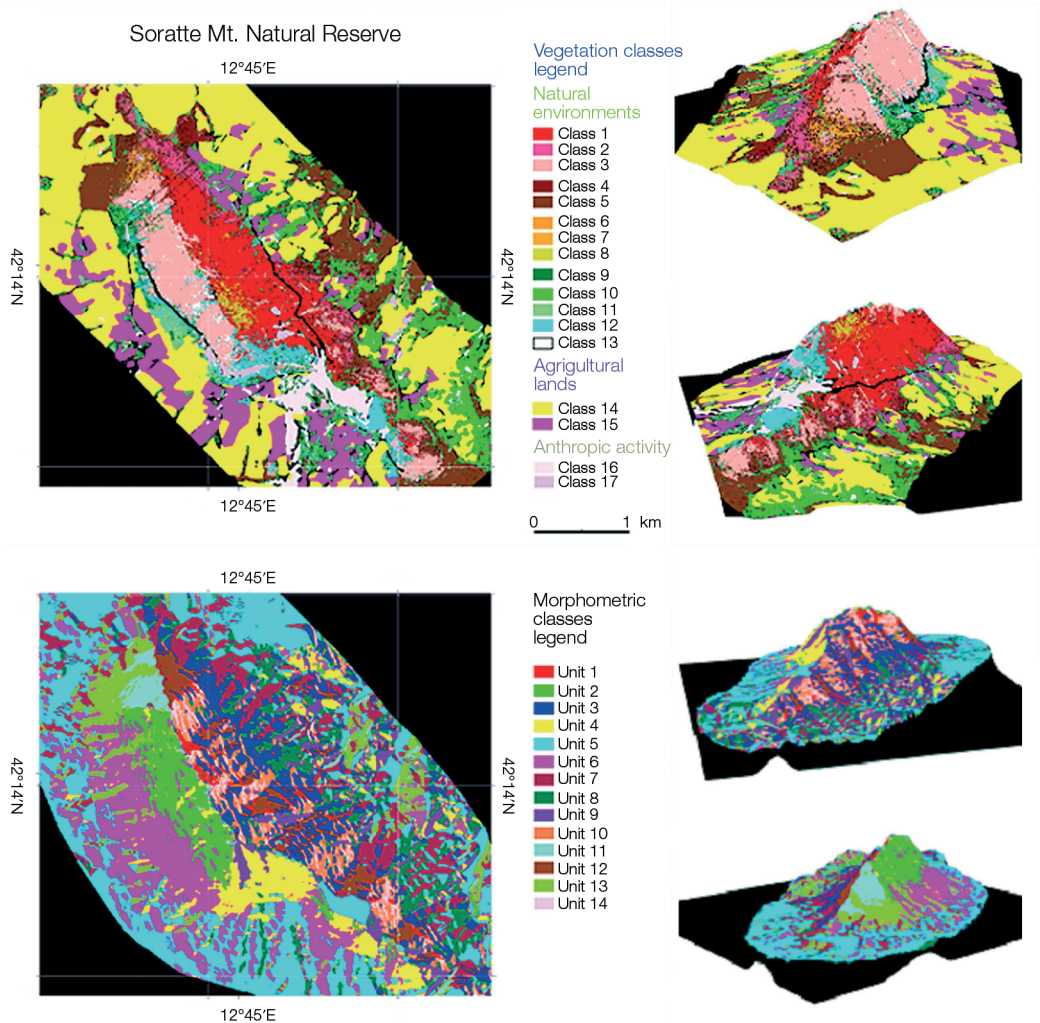


Fig. 3. *Top left:* map showing the prevailing vegetation classes on Soratte Mt. as derived from the ML classification. *Top right:* two 3D perspective views of the vegetation classes map, draped over the DEM: in the former (down) the view is from South to North, in the latter (up) from north to south. *Bottom left:* map showing the results of the ISODATA classification. *Bottom right:* two 3D views of the morphometric units map, draped over the DEM: in the former (down) the view is from north to south, in the latter (up) from south to north. Vertical exaggeration of the 3D views is 2 to better enhance the overall relief.

5. Mixed deciduous broadleaf oak-woods with *Quercus cerris*, *Quercus frainetto*, *Carpinus orientalis*, *Fraxinus ornus*, *Acer campestre*.
6. *Ostrya carpinifolia* communities.
7. *Carpinus orientalis* communities.
8. *Acer monspessulanum* communities.
9. *Spartium junceum* shrublands with subordinate presence of *Helychrysum italicum* and *Pistacia terebinthus*.
10. Synanthropic herbaceous vegetation of mesic habitats (*Pteridium aquilinum*, *Solanum nigrum*, *Chenopodium album*).
11. Garigues with tall gramineae (*Helychrysum italicum*, *Dactylis glomerata*, *Dasyphyrum villosum*, subordinately *Sp. junceum*).
12. Xerophytic grasslands in arid habitats with populations of *Euphorbia characias* and *Helychrysum italicum*.
13. Fragmentary and very discontinuous rock communities (*Cymbalaria muralis*, *Ceterach officinarum*, *Micromeria juliana*).
14. Arable lands.
15. Permanent crops (olive groves, vineyards).
16. Urban areas (build-up centres, single dwellings).
17. Quarries.

All identified classes were then assembled into a unique thematic map on a 1:10.000 scale (see fig. 3) and compared with the vegetation types distribution shown in the pre-existing vegetation map (Abbate *et al.*, 1981; Lattanti *et al.*, 1981).

3.3. Morphometric units discrimination

In order to quantitatively define the relief characteristics of the study area, a procedure, based on the analysis of local morphological setting, was applied to morphometric data gathered by processing a raster DEM (10 m/pixel). It is the same procedure used to geometrically correct the MIVIS images and was obtained by interpolating contour lines of a topographic map on a 1:10.000 scale. The quantitative technique applied to process this DEM represents a new method of analysis, implemented also in other geomorphological studies (Parcharidis *et al.*, 2001; Adediran *et al.*, 2004). It is based

on the application of a multivariate statistical procedure to a 8-layers stack, describing topographic gradients measured along the 8 compass orientations of each DEM pixel neighbourhood. This makes it possible to define areas characterized by similar local morphological setting, that reveal changes in shape, orientation and steepness of the relief. The method follows the approach inherent in the unsupervised classification or the spectrum shape analysis of multispectral bands imagery. For each pixel of a DEM, the 8 neighbourhood cells values are considered as defining a trend resembling that of contiguous spectral bands (left panel of fig. 4). Therefore, the input data to the classification procedure are the eight elevation differences between each DEM's pixel and its neighbours, calculated along the 8 main azimuth orientations starting from the NW corner and moving clockwise (right panel of fig. 4). The classification method, chosen to process the resulting gradient values, has been an unsupervised cluster analysis technique, such as ISODATA. It represents a flexible, iterative partitioning method used extensively in engineering (Hall and Khanna, 1977) and based upon estimating some reasonable assignment of the pixel vectors into candidate and, then, moving them from one cluster to another in such a way that the sum of squared error (SSE) measure of the preceding section is reduced. ISODATA stands for «Iterative Self-Organizing Data Analysis Technique», and «Self-Organizing» refers to the way in which it locates the clusters that are inherent in the data. The ISODATA utility repeats the clustering of the multi-imagery until either a maximum number of iterations have been performed, or a maximum percentage of unchanged pixels have been reached between two iterations. The output of the classification is presented as a digital thematic map showing the spatial distribution of the class membership across the study area, where each class exhibits similar morphological setting.

To apply the ISODATA procedure to the Soratte Mt. area, the following input parameters were chosen: a number of 14 classes, a change threshold percent of 1.0 and a maximum iterations number of 25, but the procedure usually converges before 15 iterations. The resulting

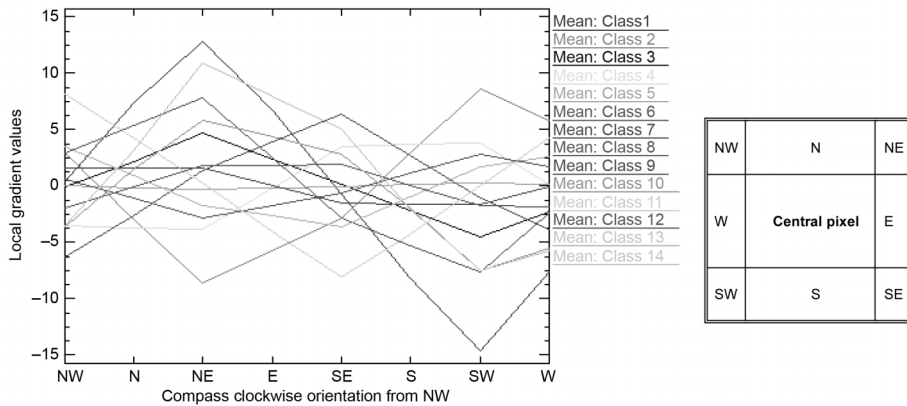


Fig. 4. Sketch of the basic concept for local morphometric analysis.

classification map was presented assigning each class a given colour shade (fig. 3) to facilitate the interpretation and to perform an accurate evaluation of the spatial distribution of different local morphological settings. The classes were then statistically analysed by computing mean and standard deviation of the eight layers, represented by the elevation differences with respect to each reference DEM’s pixel. Moreover, to verify the accuracy of the corresponding map, slope and aspect values, relative to the Soratte Mt. area, were calculated from the same elevation matrix. Then, mean and st. dev. of height, slope and aspect, relatively to all 14 ISODATA classes, were computed and compared with the 8-layers statistics earlier obtained directly from the classified thematic layers.

4. Results and discussion

4.1. Land cover classification

The analysis of the MIVIS remotely sensed data, supported by the contribution of ancillary information (gathered from field surveys and pre-existing vegetation map), made it possible to define the spectral signatures of the main plant typologies described for the territory of the Soratte Mt. natural reserve. The ML algorithm was chosen because it proved to be more

correct than other classifiers for the recognition of spectral classes, such as vegetation species, which exhibit many correlated spectra (Congalton, 1993). The decision criterion of the ML classifier is, in fact, based on the calculation of statistical parameters (average value and covariance matrix) for each training area. The ML classification yielded valuable results in the discrimination of forest, shrub and herbaceous formations, and, in particular, among the woodland types. This discrimination among different plant typologies mainly exploits the spectral differences present in the near-infrared region (Deering *et al.*, 1994) (see fig. 2): for example, the sclerophyllous communities have lower spectral responses than broadleaf ones. Overall accuracy of the ML classification results turned out to be of 94.4% and the Kappa coefficient was equal to 0.9259.

4.2. Morpho-units statistics and interpretation

The statistical results and interpretation for all 14 morphometric classes attained are shown in table III that illustrates the mean gradient values of the 8 ISODATA input layers, the average values of elevation, slope and aspect angles, and the relative morphostructural interpretation. Looking at these statistical results, it is possible to verify that the morpho-units, classi-

Table III. Altitude, slope and aspect mean values and morphostructural interpretation of the elevation differences between each pixel and the eight neighbours, for the 14 classes obtained by applying ISODATA clustering method to the study area.

Isodata units	Morphometric units interpretation	Altitude differences (m)			Altitude	Slope	Aspect
1 (1184 pixel) Red	Very steeply sloping areas facing NE-N	+0.4	+7.4	+12.8	429.7 m	44.8°	42.7°
		-7.6	-	+6.8			
		-14.7	-8.2	-0.8			
2 (8149 pixel) Green	Steeply sloping areas facing SW-W	+2.9	-2.9	-8.6	435.1 m	33.2°	243.4°
		+5.8	-	-5.8			
		+8.5	+2.9	-2.8			
3 (14458 pixel) Blue	Averagely sloping areas facing NE-E	-0.1	+2.2	+4.7	271.8 m	18.2°	47.0°
		-2.3	-	+2.4			
		-4.5	-2.1	+0.2			
4 (11017 pixel) Yellow	Averagely sloping areas facing S	-3.5	-3.7	-3.8	301.1 m	20.7°	180.9°
		+0.2	-	-0.2			
		+3.9	+3.7	+3.5			
5 (58894 pixel) Cyan	Almost flat areas facing S-SW	0	-0.1	-0.3	195.7 m	3.2°	200.1°
		+0.1	-	-0.1			
		+0.3	+0.1	0			
6 (28150 pixel) Magenta	Gently sloping areas facing SW-W	+0.6	-1.1	-2.8	254.6 m	12.2°	237.6°
		+1.7	-	-1.7			
		+2.8	+1.1	-0.6			
7 (21752 pixel) Maroon	Very gently sloping areas facing S	+1.5	+1.6	+1.6	184.1 m	9.9°	180.0°
		0	-	0			
		-1.6	-1.6	-1.6			
8 (19907 pixel) Sea green	Gently sloping areas facing E	-1.9	-0.1	+1.7	198.1 m	11.4°	91.6°
		-1.8	-	+1.9			
		-1.8	+0.1	+1.9			
9 (5843 pixel) Purple	Averagely-Steeply sloping areas facing SE-E	-6.2	-2.6	+1.4	245.1 m	25.1°	123.9°
		-3.8	-	+3.9			
		-1.1	+2.7	+6.3			
10 (7054 pixel) Coral	Averagely-Steeply sloping areas facing E-NE	-3.6	+1.5	+5.8	330.4 m	27.9°	71.2°
		-5.5	-	+4.4			
		-7.4	-1.9	+2.8			
11 (3042 pixel) Aqua marine	Steeply sloping areas facing NW	+8.1	+4.3	+0.3	301.6 m	30.6°	316.8°
		+1.2	-	-4.0			
		0	-4.3	-8.1			
12 (6762 pixel) Sienna	Steeply sloping areas facing NE	+2.9	+5.4	+7.8	323.1 m	30.7°	43.1°
		-2.4	-	+2.4			
		-7.6	-5.3	-2.9			
13 (11936 pixel) Chartreuse	Averagely sloping areas facing W-NW	+3.5	+0.9	-1.7	218.4 m	16.1°	290.4°
		+2.6	-	-2.6			
		+1.7	-0.9	-3.6			
14 (2990 pixel) Thistle	Very steeply sloping areas facing E-NE	-3.5	+3.2	+11	371.4 m	36.2°	69.0°
		-5.8	-	+8			
		-7.5	-2.1	+5			

fied on the basis of local topographic gradient, seems to be differentiated also considering elevation, aspect and slope. For instance, gently sloping areas with aspect towards to South-West/West (class 6) is in a different class from steeply sloping areas facing South-West/West (class 2). Class centroid means of component terrain derivatives (elevation, aspect and slope) were further used to interpret similarities and differences between classes (see table III). For example class 1 is similar, in terms of aspect values, to class 12 and class 3 (42.7° with respect to 43.1° and 47°), even though the first class is higher (430 m with respect to 323 m and 272 m) and steeper (44.8° instead of 30.7° and 18.2°) than the other two. Classes 4 and 7 exhibit analogous trend: both with mean aspect value of 180°, but the former presents higher mean height (301 m instead of 184 m) and average slope (21° instead of 10°) values. Finally, the comparison between class 10 and 14 depicts a quite interesting scenario: the two classes exhibit similar mean values of elevation, slope and aspect, but looking at their local morphological settings (see table III) appear different: in fact, class 10 is steeper uphill than downhill, while class 14 is steeper downhill than uphill, determining respectively morphological concave and convex forms.

4.3. Correlation between land cover types and morphological units

In order to obtain the relation between morphometric units and land cover types, a correspondence analysis was performed (Hoersch, 2003).

i) A preliminary cross-tabulation table was computed to show the number of pixels for each class as obtained from both the morphometric and land cover maps. Then, the percent occurrence of the different land cover types within each morpho-unit was calculated by standardizing the corresponding absolute representative pixels number with respect to the total number of pixels of the considered morpho-unit (see table IV).

ii) Furthermore, the distribution of the dominance land cover types within all the morpho-

metric units was assessed. Table V shows this correspondence between the morphometric units and the relative dominance land cover types.

The spatial distribution of the different ISO-DATA classes and their correlation to the land cover types were examined and shown in the tables IV and V. Looking at table IV it is evident that class 14 (*arable lands*) is the most present land cover type in many morpho-units; moreover, mixed sclerophylls thickets with deciduous species (class 3) and Mediterranean evergreen sclerophylls woods with predominance of *Quercus ilex* (class 1) are also quite abundant in the morphometric units. The analysis of table V presents a different interpretation key allowing to determine peculiar morphological characteristics related to land cover types: class 7 (*Carpinus orientalis* communities) is strongly correlated to morphometric class 11 (steeply sloping areas facing NW). Other remarkable links occur between: land cover class 3 (*mixed sclerophylls thickets with deciduous species*) and morpho-unit #2 (steeply sloping areas facing SW-W); land cover 8 (*Acer monspessulanum* communities) and morpho-unit #10 (averagely-steeply sloping areas facing E-NE); land cover 6 (*Ostrya carpinifolia* communities) and morpho-unit #3 (averagely sloping areas facing NE-E). It has been also observed that in morphometric unit#1 (very steeply sloping areas facing NE-N) the most abundant land cover types is class 3 (mixed sclerophylls thickets with deciduous species), while in morpho-unit#5 (almost flat areas facing S-SW) the dominant land cover is class 16 (*urban areas*).

The extracted mutual relations highlight the effect induced on the vegetation spatial distribution by the sun exposition and irradiation (light and heat) and by the geomorphological characteristics, responsible for a major or minor evaporation-transpiration of the soils and plants. As shown in table V, on the steeply sloping areas facing SW-W (class 2 of the morpho-units) of the Soratte Mt. area, where the soils undergo erosion processes and exhibit scarce thickness (Lulli *et al.*, 1988), the sclerophylls thickets (class 3 of the vegetation types) are abundant and constituted by *thermophilus* species that need lower water contribution. In-

Table IV. Relative distribution of the 17 land cover types within each of the 14 morpho-units.

Isodata ML	CL 1	CL 2	CL 3	CL 4	CL 5	CL 6	CL 7	CL 8	CL 9	CL 10	CL 11	CL 12	CL 13	CL 14
CL 1	0.2838	0.0000	0.2885	0.0119	0.0047	0.0010	0.0115	0.0580	0.1356	0.4815	0.0171	0.3141	0.0019	0.4700
CL 2	0.0869	0.0051	0.0644	0.0106	0.0121	0.0126	0.0265	0.0192	0.0298	0.0568	0.0745	0.1693	0.0391	0.0518
CL 3	0.4342	0.6603	0.0365	0.1256	0.0074	0.0343	0.0037	0.0124	0.0983	0.0793	0.4471	0.1455	0.1036	0.1526
CL 4	0.0005	0.0000	0.0091	0.0013	0.0060	0.0004	0.0328	0.0111	0.0085	0.0040	0.0006	0.0031	0.0025	0.0026
CL 5	0.0861	0.0203	0.1059	0.0445	0.0737	0.0302	0.1142	0.0749	0.1571	0.0882	0.2075	0.1660	0.2994	0.0893
CL 6	0.0000	0.0000	0.0049	0.0000	0.0000	0.0000	0.0002	0.0002	0.0001	0.0027	0.0000	0.0034	0.0000	0.0033
CL 7	0.0141	0.0001	0.0022	0.0004	0.0014	0.0008	0.0042	0.0009	0.0013	0.0018	0.1201	0.0202	0.0237	0.0030
CL 8	0.0015	0.0000	0.0364	0.0000	0.0002	0.0000	0.0002	0.0072	0.0041	0.0493	0.0000	0.0032	0.0000	0.0371
CL 9	0.0023	0.0113	0.0184	0.0261	0.0117	0.0272	0.0155	0.0142	0.0164	0.0066	0.0048	0.0118	0.0220	0.0067
CL 10	0.0491	0.0398	0.1399	0.1012	0.0722	0.0491	0.1468	0.1439	0.1371	0.0892	0.0702	0.0939	0.0939	0.0759
CL 11	0.0018	0.0245	0.0058	0.0198	0.0112	0.0364	0.0077	0.0156	0.0072	0.0020	0.0044	0.0013	0.0131	0.0009
CL 12	0.0071	0.0755	0.0147	0.1872	0.0119	0.0529	0.0039	0.0177	0.1261	0.0403	0.0022	0.0061	0.0170	0.0343
CL 13	0.0116	0.1007	0.0151	0.0767	0.0104	0.0130	0.0104	0.0158	0.0357	0.0121	0.0064	0.0046	0.0069	0.0139
CL 14	<u>0.0169</u>	<u>0.0132</u>	<u>0.1575</u>	<u>0.1420</u>	0.5728	<u>0.4101</u>	0.5516	0.4716	<u>0.1659</u>	<u>0.0486</u>	<u>0.0276</u>	<u>0.0332</u>	<u>0.2959</u>	<u>0.0347</u>
CL 15	0.0033	0.0006	0.0926	0.1567	0.1206	0.2953	0.0579	0.1090	0.0314	0.0088	0.0162	0.0096	0.0706	0.0035
CL 16	0.0000	0.0074	0.0037	0.0683	0.0792	0.0279	0.0023	0.0237	0.0172	0.0257	0.0000	0.0023	0.0045	0.0187
CL 17	0.0010	0.0414	0.0046	0.0278	0.0047	0.0089	0.0107	0.0047	0.0282	0.0032	0.0014	0.0124	0.0060	0.0018

Table V. The dominance land cover types in each and all morphological units.

Morphometric units interpretations	Prevailing land cover classes
1. Very steeply sloping areas facing NE-N.	Mediterranean sclerophylls woods with predominance of <i>Quercus ilex</i> and subordinate presence of deciduous trees (CL 1).
2. Steeply sloping areas facing SW-W.	Mixed sclerophylls thickets with deciduous species (CL 3).
3. Averagely sloping areas facing NE-E.	<i>Ostrya carpinifolia</i> communities (CL 6).
4. Averagely sloping areas facing S.	Xerophytic grasslands in arid habitats (CL 12) and fragmentary and very discontinuous rock communities (CL 13).
5. Almost flat areas facing S-SW.	Urban areas (CL 16) and arable lands (CL 14).
6. Gently sloping areas facing SW-W.	Garigues with tall gramineae (CL 11) and permanent crops (CL 15).
7. Very gently sloping areas facing S.	Deciduous broadleaf oak-woods with dominance of <i>Quercus cerris</i> and subordinately <i>Quercus frainetto</i> , <i>Carpinus orientalis</i> , <i>Fraxinus ornus</i> , <i>Acer campestre</i> , <i>Ostrya carpinifolia</i> (CL 4).
8. Gently sloping areas facing E.	Synanthropic herbaceous vegetation of mesic habitats (CL 10), arable lands (CL 14).
9. Averagely-Steeply sloping areas facing SE-E.	Xerophytic grasslands in arid habitats (CL 12) and quarries (CL 17).
10. Averagely-Steeply sloping areas facing E-NE.	<i>Acer monspessulanum</i> communities (CL 8) and (CL 1).
11. Steeply sloping areas facing NW.	<i>Carpinus orientalis</i> communities (CL 7).
12. Steeply sloping areas facing NE.	<i>Ostrya carpinifolia</i> communities (CL 6) and mixed woods with evergreen sclerophylls and deciduous trees (CL 2).
13. Averagely sloping areas facing W-NW.	<i>Carpinus orientalis</i> communities (CL 7) and mixed deciduous broadleaf oak-woods (CL 5).
14. Very steeply sloping areas facing E-NE.	Mediterranean sclerophylls woods with predominance of <i>Quercus ilex</i> and subordinate presence of deciduous trees (CL 1) and <i>Acer monspessulanum</i> communities (CL 8).

stead mixed deciduous broadleaf oak-woods with *Quercus cerris*, *Quercus frainetto*, *Carpinus orientalis*, *Fraxinus ornus*, *Acer campestre* (class 5 of the vegetation types) are dominant in the NW-W slopes, in agreement to the soils that are deeper and with a better water retention capability, also improved by the NW slope aspect. In the SW-W side at the foot of the mountain, where the thickness of the ground decreases and dryness conditions take place (class 6 of the morpho-units interpretation), the rocky substratum crops out and xerophytic grasslands and garigues (class 11 and 12 of the vegetation types) prevail.

5. Conclusions

The synergistic use of hyperspectral remote sensed data and DEMs was very helpful for the evaluation of the direct influence of the landscape morphology on the productivity of the vegetation covers. The unsupervised classification of a multilayer data set extracted from a DEM has allowed the automated definition of geomorphic units within the natural reserve of Soratte Mt. The application of this processing method for the evaluation of similar morphometric units has permitted to highlight the spatial distribution of morphologic features and their

degree of intensity, providing a valuable new information source for morphological applications. The designated landform units can be easily overlaid on any digital map and imagery for further applied research. In the context of the Soratte Mt. area, the peculiar correspondences among some vegetation categories and morpho-units may be also due to the overall good accuracy of the vegetation thematic map as obtained by applying the ML classification procedure to the MIVIS hyperspectral data set. An interesting development of the presented approach could be, for instance, the investigation of the mutual relation between morphology, geomorphology, soil, vegetation distribution and human activities impact, framed also into the natural processes and the natural hazard problems. A better understanding of this relation would also benefit the inventory of forest resources as well as the evaluation of the potential land productivity in areas of relief and of limited cartographic coverage.

REFERENCES

- ABBATE, G., G.C. AVENA., C. BLASI and L. VERI (1981): *Studio delle Tipologie Fitosociologiche del Monte Soratte e loro Contributo nella Definizione Fitogeografia dei Complessi Vegetazionali Centro-Appenninici*, Collana P.F. «Promozione della Qualità dell'Ambiente», AQ/1/125, Roma (Italy).
- ADEDIRAN, A.O., I. PARCHARIDIS, M. POSCOLIERI and K. PAVLOPOULOS (2004): Computer assisted discrimination of morphological units on North-Central Crete (Greece), by applying multivariate statistics to local relief gradients, *Geomorphology*, **58**, 357-370.
- AHMAD, W., L.B. JUPP and M. NUNEZ (1992): Land cover mapping in a rugged terrain using Landsat MSS data, *Int. J. Remote Sensing*, **13**, 673-683.
- BIANCHI, R., C.M. MARINO and S. PIGNATTI (1994): Airborne hyperspectral remote sensing in Italy, in *Proceedings of the «Recent Advances in Remote Sensing and Hyperspectral Remote Sensing»*, Rome (Italy), SPIE Proc., EUROPTO Ser., **2318**, 29-37.
- BLASI, C. (1994): Fitoclimatologia del Lazio, *Fitosociol.*, **27**, 151-175.
- BOLSTAD, P.V., W. SWANK and J. VOSE (1998): Predicting Southern Appalachian over story vegetation with digital terrain data, *Landscape Ecol.*, **13**, 271-283.
- CONGALTON, R.G., K. GREEN and J. TEPLY (1993): Mapping old-growth forest on National Forests and park lands in the Pacific Northwest from remotely sensed data, *Photogramm. Eng. Remote Sensing*, **59** (5), 529-535.
- DEERING, D.W., E.M. MIDDLETON and T.F. ECK (1994): Reflectance anisotropy for spruce-hemlock forest canopy, *Remote Sensing Environ.*, **47**, 242-260.
- EKSTRAND, S. (1993): Assessment of forest damage with Landsat TM, elevation models and digital forest maps, *Ph.D. Thesis* (Royal Institute of Technology, Stockholm, Sweden).
- GILES, P.T. and S.E. FRANKLIN (1998): An automated approach to the classification of the slope units using digital data, *Geomorphology*, **21**, 251-264.
- HALL, D.J. and D. KHANNA (1977): *Statistical Methods for Digital Computers* (John Wiley & Sons, New York).
- HOERSCH, B. (2003): Modelling the spatial distribution of montane and sub-alpine forests in the Central Alps using digital elevation models, *Ecol. Modeling*, **168**, 267-282.
- HOERSCH, B., G. BRAUN and U. SCHMIDT (2002): Relation between landform and vegetation in alpine regions of Wallis, Switzerland. A multi-scale remote sensing and GIS approach, *Comput. Environ. Urban Syst.*, **26**, 113-139.
- HUTCHINSON, M.F. and J.C. GALLANT (2000): Digital elevation models and representation of terrain shape, in *Terrain Analysis: Principles and Applications*, edited by J.P. WILSON and J.C. GALLANT (Wiley, New York), 29-49.
- IGM (1954): *Volo Italia, Volo GAI*, IGMI and «Gruppo Aereo Italiano» Company, 1954-55.
- LATTANTI, E. and M.L. LEPORATTI GREGORIO (1981): Contributo alla conoscenza della flora del Monte Soratte (Lazio), *Ann. Bot.*, **XXXIX** (2), 197-225.
- LULLI, L., G. DOWGIALLO and L. BRUNELLI (1988): I suoli dei rilievi del M. Soratte e M. Piccolo (Lazio) e la loro influenza sulla vegetazione, *Ann. Ist. Sper. Studio Difesa Suolo*, **XIX**, 85-107.
- NOGAMI, M. (1995): Geomorphometric measures for digital elevation models, *Z. Geomorphol.*, **101**, 53-67.
- ONORATI, G., M. POSCOLIERI, R. VENTURA, V. CHIARINI and U. CRUCILLA (1992): Analysis of the Digital Elevation Model of Italy for quantitative geomorphology and structural geology, *Catena*, **19**, 147-178.
- PIGNATTI, S. (1982): *Flora d'Italia* (Ed. Agricole, Bologna, Italy), 3 vols.
- PIKE, R.J. (2002): A bibliography of terrain modelling (geomorphometry), the quantitative representation of topography, *U.S. Geol. Surv. Open-File Rep. 02-465*.
- ROGANA, J., J. FRANKLIN and A. DAR ROBERTS (2002): A comparison of methods for monitoring multitemporal vegetation change using thematic mapper imagery, *Remote Sensing Environ.*, **80**, 143-156.
- RSI (2003): *ENVI 4.0* (Research Systems, Inc., Boulder, Colorado).
- SERVIZIO GEOLOGICO D'ITALIA (1975): *Note Illustrative della Carta Geologica d'Italia*, Fogli 138-144, Terni-Palombara Sabina, p. 16.
- TEILLET, P.M., B. GUINDON and D.G. GOODENOUGH (1982): On the slope-aspect correction of multispectral scanner data, *Can. J. Remote Sensing*, **8** (2), 829-840.
- THOMSON, A.G. and C. JONES (1990): Effects of topography on radiance from upland vegetation in North Wales, *Int. J. Remote Sensing*, **11** (5), 829-840.
- WOOD, J.D. (1996): The geomorphological characterization of digital elevation models, *Ph.D. Dissertation* (University of Leicester, U.K.).
- WYATT, B.K. (2000): Vegetation mapping from ground, air and space-competitive or complementary techniques. in *Vegetation Mapping From Patch to Planet*, edited by R.W. ALEXANDER and A.C. MILLINGTON (John Wiley & Sons Ltd., Chichester, U.K.), 3-18.